Ledeen, R. W.; Hogan, E. L.; Tettamanti, G.; Yates, A. J.; Yu, R. K., Eds.; Liviana Press: Padova, Italy, 1988.
5. Sachinidis, A.; Kraus, R.; Seul, C.; Meyer, Z.; Brickwedde, M. K.; Schulte, K.; Ko, Y.; Hoppe, J.; Veter, H. *Eur. J. Cell Biol.* **1996**, *71*, 70.
6. Silva, R. H.; Felicio, L. F.; Nasello, A. G.; Viral, M. A. B. F.; Frussa, F. R. *J. Aging.* **1996**, *17*, 583.
7. Hakomori, S. I. *J. Biol. Chem.* **1990**, *265*, 18713.
8. Brennan, M. J.; Hannah, J. H.; Leininger, E. *J. Biol. Chem.* **1991**, *266*, 18827.
9. Yu, L.; Lee, K. K.; Hodges, R. S.; Paranchych, W.; Irvin, R. *Infect. Immun.* **1994**, *62*, 5213.
10. Imundo, L.; Barasch, J.; Prince, A.; Al, A. Q. *Proc. Natl. Acad. Sci. USA* **1995**, *92*, 3019.
11. Yu, L.; Lee, K. K.; Sheth, B.; Lane-Bell, P.; Seivastava, G.; Hindsgaul, O.; Paranchych, W.; Hodges, R. S.; Irvin, R. T. *Infect. Immun.* **1994**, *62*, 2843.
12. Acquotti, D.; Poppe, L.; Dabrowski, J.; Lieth, C.; Sonnino, S.; Tettamanti, G. *J. Am. Chem. Soc.* **1990**, *112*, 7772.
13. Acquotti, D.; Fronza, G.; Ragg, E.; Sonnino, S. *Chem. Phys. Lipids* **1991**, *59*, 107.
14. Sabesan, S.; Duus, J. O.; Fukunaga, T.; Bock, K.; Ludvigsen, S. *J. Am. Chem. Soc.* **1991**, *113*, 3236.
15. Scarsdale, J. N.; Prestegard, J. H.; Yu, R. *Biochemistry* **1990**, *29*, 9843.
16. Siebert, H.; Reuter, G.; Schauer, R.; Lieth, C.; Dabrowski, J. *Biochemistry* **1992**, *31*, 6962.
17. Lee, K.; Jhon, G.; Rhyu, G.; Bang, E.; Choi, B.; Kim, Y. *Bull. Korean Chem. Soc.* **1995**, *16*, 864.
18. Oh, J.; Kim, Y.; Won, Y. *Bull. Korean Chem. Soc.* **1995**, *16*, 1153.
19. Shim, G.; Lee, S.; Kim, Y. *Bull. Korean Chem. Soc.* **1997**, *18*, 415.
20. Bevilacqua, V. L.; Kim, Y.; Prestegard, J. H. *Biochemistry* **1992**, *31*, 9339.
21. Lee, K.; Kim, Y. *Bull. Korean Chem. Soc.* **1996**, *17*, 118.
22. Bax, A.; Davis, D. G. *J. Magn. Reson.* **1985**, *65*, 355.
23. Macura, S.; Ernst, R. R. *Mol. Phys.* **1980**, *41*, 95.
24. Derome, A.; Willamson, M. *J. Magn. Reson.* **1990**, *88*, 177.
25. Bax, A. Davis, D. G. *J. Magn. Reson.* **1985**, *63*, 207.
26. Molecular Simulations Inc., San Diego, CA, USA.
27. Havel, T. F. *Prog. Biophys. Mol. Biol.* **1991**, *56*, 43.
28. Homans, S. W. *Biochemistry* **1990**, *29*, 9110.
29. Park, H.; Jhon, G.; Han, S.; Kang, Y. *Biopolymers* **1997**, *42*, 19.

Luminescence, Excitation and Far-Infrared Spectroscopy of *cis*-α-Dichlorotriethyleneteraminechromium(III) Chloride

Jong-Ha Choi

Department of Chemistry, Andong National University, Andong 760-749, Korea
Received February 19, 1998

The 77 K luminescence and excitation spectra, and 298 K infrared and absorption spectra of *cis*-α-[Cr(trien)Cl$_2$]Cl·H$_2$O (trien=triethylenetetramine) have been measured. Ligand field electronic transitions due to spin-allowed and spin-forbidden are assigned. The zero-phonon line in the excitation spectrum splits into two components by 198 cm^{-1}, and the large ^2E_g splitting can be reproduced by the modern ligand field theory. It is confirmed that nitrogen atoms of the trien ligand have a strong σ-donor character, but chloride ligand has weak σ- and π-donor properties toward chromium(III) ion.

Introduction

The synthesis, kinetics of aquation, absorption and infrared spectral data and ligand field photolysis of the dichlorochromium(III) complex containing linear quadridentate triethylenetetramine (trien=2,2,2-tet) ligand have been studied.[1-3] However, the vibrational and electronic energy levels based on the luminescence and excitation spectroscopy of title complex have not been known yet. The sharp-line electronic spectroscopic techniques offer promise in obtaining geometric informations, especially in noncrystalline environments, and in determining metal-ligand bonding properties.[4,5]

In this study the luminescence, excitation and infrared spectra of *cis*-α-[Cr(trien)Cl$_2$]Cl H$_2$O were measured. The vibrational intervals of the electronic state were determined from the far-infrared and luminescence spectra. The pure electronic origins were assigned by analyzing the absorption and excitation spectra. Using observed electronic transitions, a ligand field analysis has been performed to determine the detailed bonding properties for the coordinated chloride and nitrogen atoms toward chromium(III) ion.

Experimental Section

Anhydrous chromium(III) chloride and ligand trien (Aldrich, technical grade) were used without further purification. All other commercially available chemicals were reagent grade. The *cis*-α-[Cr(trien)Cl$_2$]Cl·H$_2$O was prepared according to the published method.[1] The measured visible

absorption maxima were in good agreement with the values reported there. Before the spectra were recorded, the compound was purified by recrystallization.

The 77 K luminescence and excitation spectra of microcrystalline sample were measured on a Spex Fluorolog-2 FL212 spectrofluorometer under the conditions previously described in details.[6] The mid-infrared spectrum was obtained with a Mattson Infinities series FT-IR spectrometer using a KBr pellet. The far-infrared spectrum was recorded with a Bruker 113V spectrometer. The compound was pressed into a polyethylene pellet (concentration 2 mg in 100 mg polyethylene) by using a Spex 3624B X-Press. The room temperature visible absorption spectrum was recorded with a Hewlett-Packard 8452A diode array spectrophotometer.

Results and Discussion

Vibrational Intervals. The far-infrared spectrum of *cis*-α-[Cr(trien)Cl_2]Cl·H_2O recorded at room temperature are presented in Figure 1.

The strong peaks at 457 and 471 cm^{-1} can be assigned to the Cr-N stretching mode. A number of absorption bands below 349 cm^{-1} arise from lattice vibration, skeletal bending and the Cr-Cl stretching mode. The vibrational intervals of the electronic ground state can be obtained by comparing the luminescence spectrum with far-infrared spectral data.

The 530 nm excited 77 K luminescence spectrum of *cis*-α-[Cr(trien)Cl_2]Cl·H_2O is shown in Figure 2. The band positions relative to the lowest zero phonon line, R_1, with corresponding infrared frequencies, are listed in Table 1. The vibrational fine structure of the ground state is observed. The luminescence spectrum except the overall intensities did not vary with exciting wavelength within the first spin-allowed transition region.

The strongest peak at 14170 cm^{-1} is assigned as the zero-phonon line, R_1, because a corresponding strong peak is found at 14174 cm^{-1} in the excitation spectrum. A well defined hot band at 14302 cm^{-1} may be assigned to the second component of the $^2E_g \rightarrow {}^4A_{2g}$ transition. The vibronic intervals occurring in the spectrum consist of several modes that can be presumed to involve primarily lattice vibration and ring torsion modes in the range 56-205 cm^{-1}. The N-Cr-N bending modes can be assigned to the 244 and 268 cm^{-1}. The Cr-N stretching mode was observed at 469

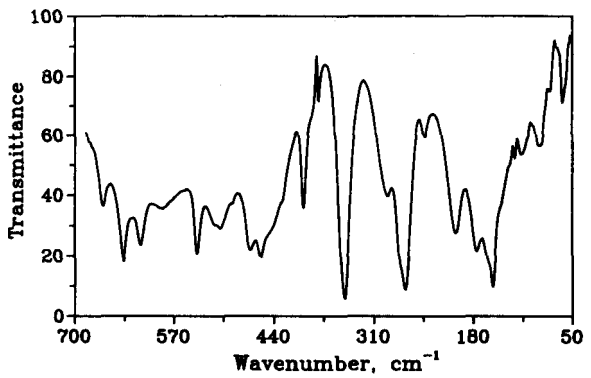

Figure 1. Far-infrared spectrum of microcrystal *cis*-α-[Cr(trien)Cl_2]Cl·H_2O at 298 K.

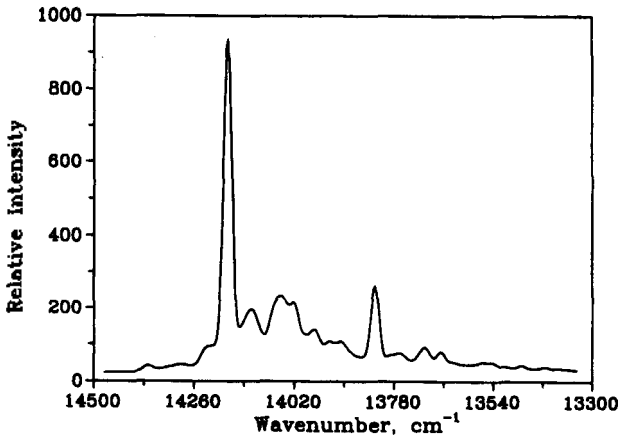

Figure 2. The 77 K luminescence spectrum of microcrystal *cis*-α-[Cr(trien)Cl_2]Cl·H_2O (λ_{ex}=530 nm).

Table 1. Vibrational frequencies from the 77 K luminescence and 298 K infrared spectra for *cis*-α-[Cr(trien)Cl_2]Cl·H_2O (cm^{-1})

Luminescence[a]	Infrared	Assignment
−192 m		R_2
0 vs		R_1
56 m	63 m, 92 w	Lattice vib., and ring def.
127 m	118 m, 123 w	
155 w	155 s, 176 m	
205 w	202 m	
244 vw	245 vw	δ(N-Cr-N)
268 w	269 vs, 293 vw	
352 vs	349 vs	ν(Cr-Cl)
409 vw	402 m	ν(Cr-N) and ring def.
469 m	457 m, 471 m	
511 w	509 w	
	540 s	
611 vw	613 m	
633 vw	636 s, 653 w	
706 w	702 wbr	
763 vw	730 m, 762 m, 785 m	ρ(CH_2)
	812 w	
	860 m, 886 m	ρ(NH_2)

[a] Measured from zero-phonon line at 14170 cm^{-1}.

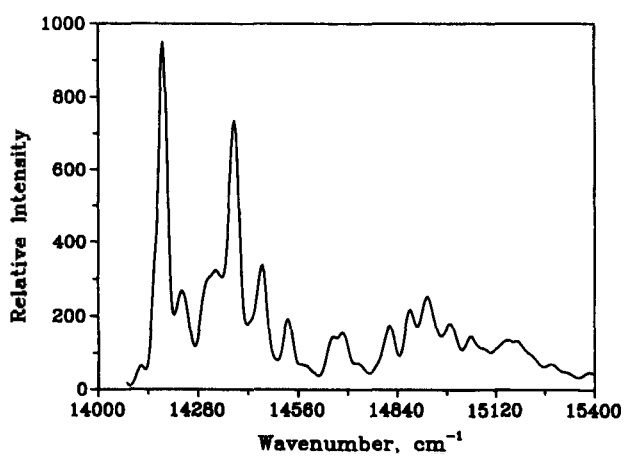

Figure 3. The 77 K excitation spectrum of microcrystal *cis*-α-[Cr(trien)Cl_2]Cl·H_2O (λ_{em}=723 nm).

cm^{-1}.[7]

Spin-forbidden Transitions. The 77 K excitation spectrum is shown in Figure 3. The spectrum was obtained by monitoring the luminescence intensity of the no phonon or the vibronic sidebands at 723 nm. The shape and peak maxima of the spectrum was independent of the vibronic peak used to monitor it. The peak positions and their assignments are tabulated in Table 2. The calculated frequencies were obtained by using the frequency values of vibrational modes ν_1-ν_5 listed in Table 2.

Two strong peaks at 14174 and 14372 cm^{-1} in the excitation spectrum are assigned to the two components (R_1 and R_2) of the $^4A_{2g} \rightarrow {}^2E_g$ transition. The lowest-energy zero-phonon line coincides with the emission origin within 4 cm^{-1}. The zero-phonon line in the excitation spectrum splits into two components by 198 cm^{-1}, and it is comparable to values for other tetragonal chromium(III) complexes.[8] In general, it is not easy to locate positions of the other electronic components because the vibronic sidebands of the ^2E_g levels overlap with the zero phonon lines of $^2T_{1g}$. However, the three components of the $^4A_{2g} \rightarrow {}^2T_{1g}$ electronic origin (T_1, T_2 and T_3) are assigned to relative intense peaks at 696, 745 and 967 cm^{-1} from the lowest electronic line, R_1 because they have no correspondence in luminescence. Vibronic satellites based on these origins also have similar frequencies and intensity patterns to those of the ^2E_g components.

The higher energy $^4A_{2g} \rightarrow {}^2T_{2g}$ band was found at 20790 cm^{-1} from the second derivative of the solution absorption spectrum, as shown with dotted line in Figure 4. It could not be resolved into the separate components.

Table 2. Assignment of sharp-line positions in the 77 K excitation spectrum of *cis*-α-[Cr(trien)Cl$_2$]Cl·H$_2$O (cm^{-1})

$\bar{\nu}_n$-14174		Assignment	Calcd[a]		Vibronic frequencies[b]	Ground state frequencies[c]
0	vs	R_1		ν_1	60	63
55	m	$R_1+\nu_1$	60	ν_2	120	155
126	sh	$R_1+2\nu_1$	120	ν_3	282	293
146	w	$R_1+\nu_2$	162	ν_4	348	349
198	vs	R_2		ν_5	457	457
279	s	$R_1+\nu_3$	282			
350	m	$R_2+\nu_2$	360			
401	w	$R_1+\nu_1+\nu_4$	408			
478	m	$R_2+\nu_3$	480			
504	m	$R_1+\nu_2+\nu_4$	510			
543	sh	$R_2+\nu_4$	546			
639	m	$R_2+\nu_3+\nu_4$	630			
696	s	T_1				
745	vs	T_2				
807	m	$T_2+\nu_1$	805			
866	w	$T_1+\nu_2$	858			
907	vw	$T_2+\nu_2$	907			
967	m	T_3				
1042	sh	$T_3+\nu_1$	1027			
1096	w	$T_2+\nu_4$	1093			
1145	vw	$T_1+\nu_5$	1153			
1204	w	$T_2+\nu_5$	1202			
1303	vw	$T_3+\nu_4$	1315			
1390	vw	$T_1+2\nu_4$	1392			

[a] Values represent the calculated frequencies based on the vibrational modes listed. [b] From the excitation spectrum. [c] From the luminescence and infared spectra.

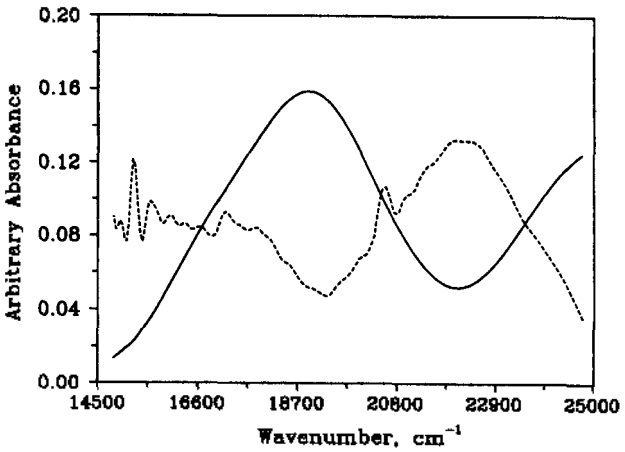

Figure 4. Absorption spectrum (solid line) and second derivative (dotted line) of *cis*-α-[Cr(trien)Cl$_2$]$^+$ in aqueous solution.

Spin-allowed Transitions. The visible absorption spectrum (solid line) of *cis*-α-[Cr(trien)Cl$_2$]$^+$ in aqueous solution at room temperature is represented in Figure 5.

It exhibits two bands, one at 18795 cm^{-1} (ν_1) and the other at 25190 cm^{-1} (ν_2), corresponding to the $^4A_{2g} \rightarrow {}^4T_{2g}$ and $^4A_{2g} \rightarrow {}^4T_{1g}$ (O_h) transitions, respectively.[9] The dotted lines represent the result of Gaussian analysis. The second quartet band has nearly symmetric profiles. However, in order to obtain some points of reference for the splittings of the two bands, the band profiles were fitted by using four Gaussian curves. A deconvolution procedure on the experimental band pattern yielded four maxima at 16745, 19090, 24790 and 25860 cm^{-1} for the noncubic splittings of $^4T_{2g}$ and $^4T_{1g}$. These resolved peak positions were adapted for the spin-allowed transition energies in the ligand field optimization.

Ligand Field Calculations. The ligand field potential matrix was generated for *cis*-[Cr(trien)Cl$_2$]$^+$ from the coordinated four nitrogen and two chloride atoms. No crystal structure for any salt of the complex ion has been known, thus the positional parameters were adapted from the *cis*-[Cr(2,2,3-tet)Cl$_2$]$^+$, replacing 2,2,3-tet with 2,2,2-tet ligand.[10]

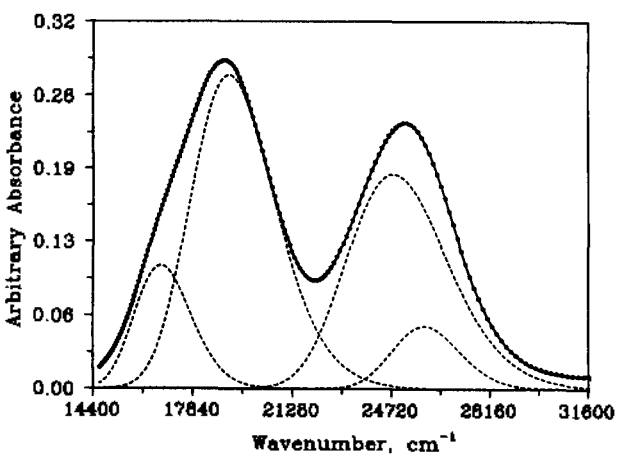

Figure 5. Electronic absorption spectrum of *cis*-α-[Cr(trien)Cl$_2$]$^+$ in aqueous solution at 298 K.

The coordinates were then rotated so as to maximize the projections of the six-coordinated atoms on the Cartesian axes centered on the chromium.

Angular overlap model (AOM) parameters provide better chemical insights than crystal field parameters, and was used to interpret the electronic spectra.[11] The ligand field analysis was carried out through an optimized fit of experimental to calculated transition energies. Diagonalization of the 120×120 secular matrix yields the doublet and quartet energies with the appropriate degeneracies.[12] The methods for determining the eigenvalues and eigenfunctions of a d^3 ion in a ligand field from any number of coordinated atoms has been described.[13] The full set of 120 single-term antisymmetrized product wavefunctions was employed as a basis. The Hamiltonian used in the calculation was

$$H = \sum_{i<j} \frac{e^2}{r_{ij}} + V_{LF} + \zeta \sum_i l_i \cdot s_i + \alpha_T \sum_i l_i^2 + 2\alpha_T \sum_{i<j} l_i \cdot l_j \qquad (1)$$

where the terms in the right-hand side represent the interelectronic repulsion, ligand field potential, and spin-orbit coupling, respectively, with the last two representing the Trees correction.[14] The parameters varied during the optimization were the interelectronic repulsion parameters B, C and the Trees correction parameter α_T, the spin-orbit coupling parameter ζ, the AOM parameters e_σ(Cl) and e_π(Cl) for the chloride-chromium, and e_σ(N) for the trien nitrogen-chromium. The π-interaction of amine nitrogens with sp^3 hybridization in the trien was assumed to be negligible. However, it is noteworthy that the peptide nitrogen with sp^2 hybridization has a weak π-donor character.[15] Schmidtke's π-expansion parameter τ were also included in the treatment of the interelectronic repulsion term. In Schmidtke's approximation, the electrostatic terms are modified by a factor τ for each constituent metal wavefunction that overlaps with a ligand π-orbital. The π-orbital expansion parameter, τ was fixed at the value 0.992. The estimated value was based on the analysis of $[Cr(NH_3)_5Cl]Cl_2$.[16] The Racah parameter, A was also fixed at 5000 cm^{-1}. The value of the Racah parameter, A has little effect on the calculated transition energies. All parameters, except e_σ(Cl) and e_π(Cl), were constrained to reasonable limits based on the data from other chromium(III) complexes.[11] The seven parameters were used to fit eleven experimental energies: the five $^4A_{2g} \rightarrow \{^2E_g, {}^2T_{1g}\}$ components, identified in Table 3, the average energy of the transition to the $^2T_{2g}$ state, the four $^4A_{2g} \rightarrow \{^4T_{2g}, {}^4T_{1g}\}$ components, and the splitting of the ^2E_g state. Eigenvalues were assigned to states within the doublet and quartet manifolds based on an analysis of the corresponding eigenfunctions. The function minimized was

$$f = 10^3 S^2 + 10^2 \sum D^2 + 10\, T^2 + \sum Q^2 \qquad (2)$$

where S in the first term is the ^2E_g splitting, and D, T, and Q represent the differences between experimental and calculated $\{^2E_g, {}^2T_{1g}\}$, $^2T_{2g}$, and $\{^4T_{2g}, {}^4T_{1g}\}$ transition energies, respectively. The Powell parallel subspace optimization procedure[17] was applied to find the global minimum. The optimization was repeated several times with different sets of starting parameters to verify that the same global minimum was found. The results of the optimization and the parameter set used to generate the best-fit energies are also listed in Table 3. This procedure proved to show good fit for the sharp line transitions. The error margins reported for the best-fit parameters in Table 3 are based only on the propagation of the assumed uncertainties in the observed peak positions.[18] The quartet terms were given a very low weight to reflect the very large uncertainty in their position.

Table 3. Experimental and calculated electronic transition energies for *cis*-α-$[Cr(trien)Cl_2]Cl \cdot H_2O$ (cm^{-1})

State (O_h)	Exptl	Calcd[a]
^2E_g	14174	14173
	14372	14370
$^2T_{1g}$	14870	14843
	14919	14974
	15141	15118
$^2T_{2g}$ (avg)	20790	20782
$^4T_{2g}$	16745[b]	16890
	19090[b]	18950
$^4T_{1g}$	24790[b]	24732
	25860[b]	25990

[a] e_σ(N)=7375±16, e_σ(Cl)=5065±35, e_π(Cl)=849±20, B=773±2, C=2614±6, α_T=171±2, ζ=198±18. [b] Obtained from the Gaussian component deconvolution.

The following values were finally obtained for the ligand field parameters: e_σ(N)=7375±16, e_σ(Cl)=5065±35, e_π(Cl)=849±20, B=773±2, C=2614±6, α_T=171±2, and ζ=198±18 cm^{-1}. A ligand field analysis of the sharp-line excitation and broad-band absorption spectra indicates that the chloride is a weak σ- and π-donor. The value of 7375 cm^{-1} for e_σ(N) is quite comparable to values for other amines.[19-22] It is suggested that the four nitrogen atoms of the linear quadridentate trien ligand have strong σ-donor properties toward chromium(III) ion. The AOM parameters can be used in predicting the photolabilized ligand and the relative quantum yields of the photoinduced reaction.[23] The aim of this research is also to create a spectroscopic basis of knowledge for the development of new efficient tunable solid-state lasers. An orbital population analysis of the type used by Ceulemans and his coworkers[24] yields a configuration of $(xy)^{1.001}(z)^{0.977}(yz)^{0.979}(x^2\text{-}y^2)^{0.025}(z^2)^{0.018}$ for the lowest component of the ^2E_g state. The relative d-orbital ordering from the calculation is $E(xy)$=938 $cm^{-1} < E(xz)$=1135 $cm^{-1} < E(yz)$=1720 $cm^{-1} < E(x^2\text{-}y^2)$=18590 $cm^{-1} < E(z^2)$=20643 cm^{-1}. The value of the Racah parameter, B is about 84% of the value for a free chromium(III) ion in the gas phase. The 198 cm^{-1} of observed ^2E_g splitting in the excitation spectrum is larger than the 120 and 139 cm^{-1} of *cis*-$[Cr(en)_2Cl_2]Cl$ and *cis*-$[Cr(cyclam)Cl_2]Cl$, respectively.[25,26] It is shown that the large ^2E_g splitting can be reproduced by the modern ligand field theory. The parameter values reported here appear to be significant, as deduced on the basis of the manifold of sharp-line transitions which were obtained from the highly resolved excitation spectrum.

Acknowledgment. My sincere thanks are due to Professor T. Schönherr, University of Düsseldorf, for the opportunity to visit his laboratory and Mr. R. Linder for obtaining far-infrared spectrum. Financial support from the Korea Science & Engineering Foundation and the Deutsche Forschungsgemeinschaft are also gratefully acknowledged.

References

1. House, D. A.; Garner, C. S. *J. Am. Chem. Soc.* **1966**, *88*, 2156
2. Hsu. C. Y.; Garner, C. S. *Inorg. Chim. Acta* **1967**, *1*, 17.
3. Thompson, M. S.; Sheridan, P. S. *Inorg. Chem.* **1979**, *18*, 1580.
4. Hoggard, P. E. *Top. Curr. Chem.* **1994**, *171*, 114.
5. Choi, J. H. *Bull. Korean Chem. Soc.* **1994**, *15*, 145.
6. Choi, J. H. *Bull. Korean Chem. Soc.* **1993**, *14*, 118.
7. Choi, J. H.; Oh, I. G. *Bull. Korean Chem. Soc.* **1993**, *14*, 348.
8. Flint, C. D.; Matthews, A. P. *J. Chem. Soc., Faraday II.* **1973**, *69*, 419.
9. Lever, A. B. P. *Inorganic Electronic Spectroscopy*; Elsevier: Amsterdam, 1984.
10. House, D. A.; Turnbull, M. M. *Inorg. Chim. Acta* **1997**, *254*, 401.
11. Schönherr, T. *Top. Curr. Chem.* **1997**, *191*, 87.
12. Smith, B. T.; Boyle, J. M.; Dongarra, J. J.; Garbow, B. S.; Ikebe, Y.; Klema, V. C.; Moler, C. B. *Matrix Eigensystem Routines-EISPACK Guide*; Spring-Verlag: Berlin, 1976.
13. Hoggard, P. E. *Coord. Chem. Rev.* **1986**, *70*, 85.
14. Trees, R. E. *Phys. Rev.* **1951**, *83*, 756.
15. Choi, J. H.; Hoggard, P. E. *Polyhedron* **1992**, *11*, 2399.
16. Schmidtke, H. H.; Adamsky, H.; Schönherr, T. *Bull. Chem. Soc. Jpn.* **1988**, *61*, 59.
17. Kuester, J. L.; Mize, J. H. *Optimization Techniques with Fortran*; McGraw-Hill: New York, 1973.
18. Clifford, A. A. *Multivariate Error Analysis*; Wiley-Hasted: New York, 1973.
19. Choi, J. H. *J. Photosci.* **1996**, *3*, 43.
20. Choi, J. H.; Oh, I. G. *Bull. Korean Chem. Soc.* **1997**, *18*, 23.
21. Choi, J. H. *Bull. Korean Chem. Soc.* **1997**, *18*, 819.
22. Choi, J. H. *J. Photosci.* **1997**, *4*, 121.
23. Vanquickenborne, L. G.; Ceulemans, A. *Coord. Chem. Rev.* **1983**, *48*, 157.
24. Ceulemans, A.; Bongaerts, N.: Vanquickenborne, L. G. *Inorg. Chem.* **1987**, *26*, 1566.
25. Flint, C. D.; Matthews, A. P.; O'Grady, P. J. *J. Chem. Soc., Faraday II.* **1977**, *73*, 877.
26. Choi, J. H. *J. Korean Chem. Soc.* **1995**, *39*, 501.